Development of Aptamer for PD-L1 expression in cancer

Yun Jung Choi

Department of Medicine

The Graduate School, Yonsei University

Development of Aptamer for PD-L1 expression in cancer

Directed by Professor Won Jun Kang

The Doctoral Dissertation
submitted to the Department of Medicine,
the Graduate School of Yonsei University
in partial fulfillment of the requirements for the degree
of Doctor of Philosophy

Yun Jung Choi

December 2021

This certifies that the Doctoral Dissertation of Yun Jung Choi is approved.

Thesis Supervisor : Won Jun Kang

Thesis Committee Member#1 : Yong Bae Kim

Thesis Committee Member#2 : Jin Chul Paeng

Thesis Committee Member#3: Sang Joon Shin

Thesis Committee Member#4: Jaemoon Yang

The Graduate School
Yonsei University

December 2021

ACKNOWLEDGEMENTS

Above all, I would like to show my gratitude to my supervisor, Professor Won Jun Kang for his supervision and encouraging suggestions throughout my academic life.

I am deeply grateful to Professors Yong Bae Kim, Jin Chul Paeng, Sang Joon Shin, and Jaemoon Yang for their precious and constructive advice. I would also thank Ye Lim Cho, Ju Ri Chae, and Jun Young Park, who supported me in my research, for all their help, support, interest, and valuable hints.

Finally, I would like to give my special thanks to my parents and family members for providing me emotional support and motivation to achieve my ambition.

<TABLE OF CONTENTS>

LIST OF FIGURES

LIST OF TABLES

ABSTRACT

Development of Aptamer for PD-L1 expression in cancer

Yun Jung Choi

Department of Medicine

The Graduate School, Yonsei University

(Directed by Professor Won Jun Kang)

Background: The Program Death 1 (PD-1) receptor is an immunosuppressive receptor expressed on activated T cells, and when the ligand, which is Program Death Ligand 1 (PD-L1), binds to it, it induces an inhibitory signal. Recent studies have indicated that PD-1/PD-L1 block can increased endogenous antitumor immunity. Thus, the PD-1/PD-L1 axis may be a promising therapeutic target for cancer immunotherapy. Aptamers are oligonucleotides with high specificity and affinity for target molecules and potential candidates for molecular imaging and targeted therapy. ^{68}Ga is an attractive radionuclide that serves as a low-cost alternative to cyclotron-produced positron emission tomography (PET) radionuclides. In this study, we generated a ^{68}Ga-labeled PD-L1 aptamer and investigated its target specificity and utility for *in vivo* PET scanning.

Method: In the first part of our study, we estimated the binding affinity of three PD-L1 aptamers in PD-L1-positive (H1975 and B16F10) and negative (A549 and HT-29) tumor cells by flow cytometry and confocal microscopy. Optical imaging studies of PD-L1 aptamers were executed in H1975 tumor-bearing mice, and the aptamer with the highest binding affinity to PD-L1 positive tumors was selected. PD-L1 aptamers were radiolabeled with ^{68}Ga. PET was performed for *in vivo* imaging of the ^{68}Ga-NOTA-PD-L1 aptamer in H1975 tumor-bearing mice (PD-L1-positive cells) and A549 tumor-bearing mice (PD-L1-negative cells).

Results: Flow cytometry and confocal microscopy indicated that PD-L1 aptamers had strong binding to PD-L1-positive H1975 and B16F10 cells. In contrast, PD-L1-negative A549 and HT-29 cells showed low binding to PD-L1 aptamers. Optical imaging of H1975 tumor-bearing mice showed the highest uptake of the 2198-06-07 PD-L1 aptamer. PET of ^{68}Ga-NOTA-PD-L1 aptamers demonstrated increased uptake into PD-L1-positive H1975 tumors compared with PD-L1-negative A549 tumors.

Conclusion: We confirmed that ^{68}Ga-NOTA-PD-L1 aptamers facilitated the visualization of PD-L1 expression by *in vivo* PET scanning. These data suggest that ^{68}Ga-NOTA-PD-L1 aptamers could potentially act as tracers for imaging for PD-L1-positive cancers.

Key Words: PD-L1, aptamer, molecular imaging, ^{68}Ga, PET

Development of Aptamer for PD-L1 expression in cancer

Yun Jung Choi

Department of Medicine
The Graduate School, Yonsei University

(Directed by Professor Won Jun Kang)

I. INTRODUCTION

Immune checkpoint inhibitor therapy is a promising new branch of immunotherapy. The programmed death-1 (PD-1) receptor is an immune inhibitory receptor that appears on activated T lymphocytes, and binding to the ligand programmable death ligand-1 (PD-L1) elicits an inhibitory signal[1,2]. The interaction between PD-1 and PD-L1 can inhibit proliferation and activation of T lymphocytes, resulting in immune evasion of tumor cells[3]. Recent studies have shown that blocking the PD-1/PD-L1 pathway may enhance intrinsic anti-tumor immunity[4]. Thus, the PD-1/PD-L1 axis can be a new treatment target for cancer.

The validation of PD-L1 by biopsy and immunohistochemistry (IHC) was used to select patients for anti-PD-L1 treatment. However, PD-L1 IHC has some limitations, such as insufficient inter-assay agreement due to the heterogeneity of PD-L1 within tumor sites[5]. Furthermore, expression of PD-L1 in tumors is temporally dynamic, and repeated biopsies are often impractical, capturing these changes during treatment is difficult[6,7]. Therefore, a non-invasive technique for assessing PD-L1 expression is required to guide treatment decisions.

Aptamers are single-stranded DNA or RNA oligonucleotides generated by the systematic evolution of ligands by exponential enrichment (SELEX) technology. Aptamers have unique three-dimensional structures that result in high specificity and affinity for target molecules[8]. Therefore, they are ideal substances for detecting and measuring the expression of target molecules. Aptamers also have a

relatively small size (6–30 kDa) and negative charges, resulting in high tissue penetration, rapid renal excretion, and a high target-to-background ratio at an early time point. For these reasons, aptamers are promising candidates for molecular imaging and targeted therapy[9,10].

Molecular imaging techniques, such as positron emission tomography (PET) and single photon emission computed tomography (SPECT) facilitate the visualization of specific physiological and functional changes in biological systems[11]. Both methods have been adopted as reliable and noninvasive imaging techniques for many cancers. Several aptamer-based radiopharmaceuticals have been developed for cancer imaging. Most of these involve ^{99m}Tc-labeled SPECT scanning, and only a few studies have developed radiolabeled aptamers for PET scanning. The majority of imaging probes were developed based on small molecules by labeling with various radionuclides, such as ^{18}F, ^{68}Ga, ^{64}Cu, and ^{99m}Tc. In recent years, the clinical applications of ^{68}Ga-radiopharmaceuticals have increased. ^{68}Ga has a short half-life (68 min), high positron yield (89%), high positron energy (1899 keV), and is available from a generator[12,13]. ^{68}Ga is an attractive radionuclide; however, ^{68}Ga-labeled PD-L1 aptamers have not been previously reported.

Therefore, the aim of this study was to develop a ^{68}Ga-labeled PD-L1 aptamer and investigate its target specificity and utility for *in vivo* PET scanning.

II. MATERIALS AND METHODS

1. Cell lines and cell culture

The human non-small cell lung cancer cell lines H1975 and A549, the human melanoma cell line B16F10, and the human colorectal adenocarcinoma cell line HT-29 were purchased from the American Type Culture Collection (Manassas, VA, USA).

The PD-L1-positive cell lines H1975 and B16F10 were used as positive controls for *in vitro* experiments. A549 and HT-29 cell lines were used as negative

controls. H1975 and A549 cell lines were used for *in vitro* and *in vivo* experiments. All the cell lines were cultured in minimum essential medium supplemented with 10% fetal bovine serum (FBS) and antibiotics (100 U/ml penicillin and 100 μg/ml streptomycin). All cells were maintained in an incubator in a controlled humidified atmosphere composed of 5% CO_2 and 95% air at 37 ℃.

2. PD-L1 aptamers

PD-L1 aptamers of different lengths and properties (2198-06-01, 2198-06-07, and 2198-06-05) were purchased from Aptamer Sciences Inc. (APSCI, Pohang, Republic of Korea). The characteristics of the three aptamers are listed in Table 1. A scrambled version of the PD-L1 aptamer was used as a negative control. All the PD-L1 aptamers were discovered using the SELEX method.

Table 1. Characteristics of aptamers

	Length (mer)	Molecular weight (Da)	Kd value (nM)
2198-06-01	76	25473	17.98
2198-06-05	52	18109	8.49
2198-06-07	37	13445	0.82

3. Western blot analysis

Cells were harvested and suspended in cell lysis buffer (Invitrogen Life Technologies, Carlsbad, CA, USA) containing protease inhibitors on ice for 30 min. Cell lysates were clarified by centrifugation at 14000 rpm for 20 min at 4°C. Protein concentrations were determined using the Bradford method (Thermo Fisher Scientific, Rockford, IL, USA). For western blot analysis, 30–60 μm of protein extract from each sample was separated by 10% sodium dodecyl sulfate-polyacrylamide gel electrophoresis and transferred to nitrocellulose membranes. The membranes were probed with a PD-L1 antibody.

Glyceraldehyde 3-phosphate dehydrogenase was used as loading control. Signals were detected using an ECL chemiluminescence substrate kit (Advansta, Menlo Park, CA, USA).

4. Flow cytometry

H1975, A549, B16F10, and HT-29 cells were seeded onto Petri dishes in complete medium and grown to 80% confluence. Cells were incubated at 4°C for 30 min with the fluorescently labeled PD-L1 aptamer as a control in saline containing 1% FBS. The cells were washed in ice-cold binding buffer. After washing, cells were analyzed using a fluorescence-activated cell sorting LSR II Flow Cytometry System (Becton Dickinson, Franklin Lakes, NJ, USA). FlowJo 10.0 (TreeStar, Ashland, OR, USA) was used for data analysis and graphical output.

5. Confocal microscopy

H1975, A549 and B16F10 cells were seeded at a density of 5×10^5 on glass coverslips and treated with the 5'-Cy5-PD-L1 aptamers in 1% FBS-containing culture medium at 4°C for 30 min. After 30 min of incubation, the cells were carefully washed and mounted on slides in a mounting medium containing 4',6-diamidino-2-phenylindole (DAPI; Vector Laboratories, Inc., Burlingame, CA, USA). The fluorescent signal was detected by a Zeiss LSM-700 confocal laser scanning microscope (Carl Zeiss, Oberkochen, Germany). The excitation wavelength and emission filters were as follows: fluorescein isothiocyanate, 488 nm laser line excitation and emission BP490-555, and DAPI, 450 nm laser line excitation and emission SP490 filter.

For confocal z-stack imaging, H1975 and A549 cells were treated with 200 nM 5'-Cy5-2198-06-07 PD-L1 aptamers and incubated at 37°C in 5% CO_2 for 30 min, 1 h, 2 h, and 4 h. At the indicated time points, the cells were washed with binding buffer and fixed with 4% paraformaldehyde. Confocal z-stack images

were acquired using Zeiss LSM 770 and processed with ZEN 2010 image software.

6. Blocking assay

To confirm the specificity of the PD-L1 aptamer, blocking studies with a large excess of the 2198-06-07 PD-L1 aptamer was performed using H1975 cells. Briefly, H1975 cells were treated with 100 pmol of 2198-06-07 PD-L1 aptamer in 1% FBS-containing culture medium at 4°C for 10 min. After 10 min of incubation, the cells were carefully washed and incubated with 10 pmol 2198-06-07 PD-L1 aptamer. Flow cytometry and confocal microscopy were performed as described previously.

7. Synthesis of ^{68}Ga-NOTA-PD-L1 aptamers

Radiolabeling was performed as described previously[14] with some modifications. ^{68}Ga was eluted from a ^{68}Ge-^{68}Ga generator using 10 mL of 0.6 N HCl, purified using strong-cation exchange Chromafix cartridges (Machery-Nagel), and subsequently eluted with 1.2 mL of 5 M NaCl. Radiolabeling was performed using 2 nmol NOTA-PD-L1 aptamer in 3 M HEPES buffer (pH 4). A 100-μL fraction of ^{68}Ga was added to the NOTA-PD-L1 aptamer and incubated at room temperature. Radio-TLC analysis confirmed the quantitative radiolabeling. The NOTA-PD-L1-aptamer was purchased from Aptamer Sciences Inc. (APSCI, Pohang, Republic of Korea).

8. Animal models

All animal studies were reviewed and approved by the Institutional Animal Care and Ethics Committee of the Yonsei Laboratory Animal Research Center and were performed in accordance with the guiding principles of the Care and Use of Laboratory Animals.

Five-week-old female BALB/c nude mice were purchased from Orient Bio (Gyeonggi-do, South Korea). For the tumor model, a suspension of 1×10^6 H1975 or A549 cells in PBS was subcutaneously injected at the dorsal side of the right shoulder. We developed a dual tumour-bearing mouse model. H1975 and A549 cells were injected into the same mouse. A549 cells were injected into the right shoulder and H1975 cells in the left shoulder.

9. Optical imaging of the PD-L1 aptamer

H1975 tumor-bearing mice were injected with Cy5-PD-L1 aptamers (1 nmol) via the tail vein. *In vivo* fluorescence imaging was performed using an IVIS Spectrum® (PerkinElmer, CA, USA) with a 640-nm excitation filter.

H1975 tumor-bearing mice were sacrificed 60 min after injection for *ex vivo* imaging. The tumor, heart, lung, liver, kidney, skin, and spleen were dissected, and fluorescence imaging was performed using the IVIS Spectrum. The regions of interest (ROIs) of tumors were manually drawn and quantified using the average radiant efficiency ([photons/sec/cm^2/sr]/[μW/cm^2]).

10. *In vivo* PET scanning

For PET scanning, H1975 and A549 tumor-bearing mice were intravenously injected with 7.4 ± 0.5 MBq ^{68}Ga-NOTA-PD-L1 aptamers via the tail vein. Small-animal PET scanning was performed using an Inveon microPET scanner (Siemens Medical Solutions USA Inc., Knoxville, TN, USA).

Dynamic scanning was performed for 90 min immediately after injection. Static studies were performed 30 min after injection with an acquisition time of 60 min. The uptake of PET images was quantified based on the ROI analysis.

Three-dimensional ROIs were drawn around the edge of the tumor or organ activity based on visual inspection. The mean and maximum activities were recorded for all ROIs.

11. Biodistribution

H1975 tumor-bearing mice were injected with ^{68}Ga-NOTA-PD-L1 aptamers (7.4 ± 0.5 MBq) through the lateral tail vein. The mice were sacrificed 30 and 60 min after the injection. Normal organs and tissues, including the blood, heart, bone, liver, kidneys, spleen, muscle, stomach, small intestine, and large intestine, as well as the tumor, were collected, and radioactivity was measured using a Wizard2 2480 gamma counter (PerkinElmer, Woodbridge, Ontario, Canada) after the organs were wet-weighed. The uptake of the radiotracer in tissues was expressed in counts per minute corrected to decay and normalized to the percentage injected dose per gram (%ID/g).

12. Statistical analysis

Quantitative data were presented as the mean ± standard deviation of the mean.

III. RESULTS

1. PD-L1 expression in tumor cells.

The expression of PD-L1 in cancer cells was evaluated using western blot analysis. Western blot analysis confirmed the expression of PD-L1 in H1975 and B16F10 cells, while the negative control cell lines, A549 and HT-29, presented no signal in the corresponding retention position (Figure 1).

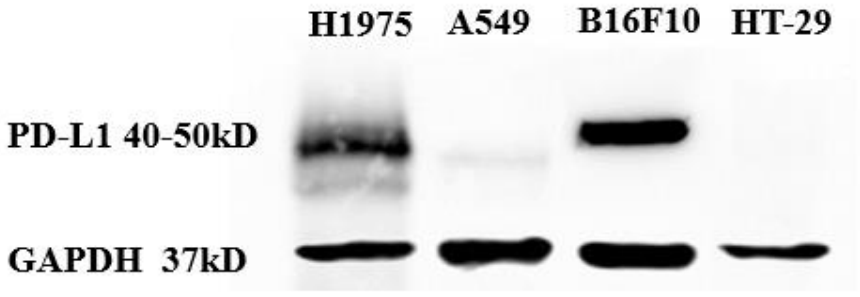

Figure 1. Evaluation of PD-L1 expression in different cancer cell lines, as determined by western blotting of cancer cell lines.

2. Binding specificity and affinity of PD-L1 aptamers

The binding affinity of PD-L1 aptamers to cancer cells was evalated using Cy5-labeled PD-L1 aptamers and analyzed by flow cytometry and confocal studies. Three aptamers with different lengths were used, including 2198-06-07 with the shortest length, 218-06-05 with medium length, and 2198-06-01 with the longest length.

Flow cytometry analysis confirmed that all PD-L1 aptamers were more strongly bound to PD-L1-positive H1975 and B16F10 cells than PD-L1-negative A549 and HT-29 cells (Figure 2). The results indicated that PD-L1 aptamers had a high affinity for PD-L1 expression cells.

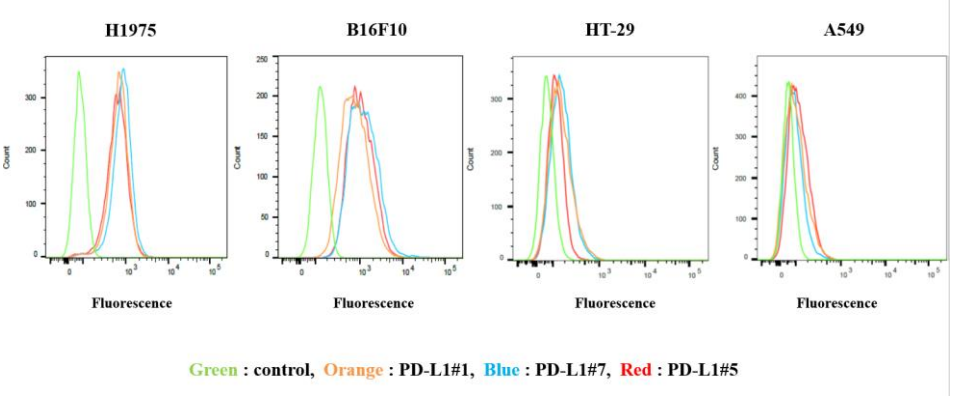

Figure 2. In vitro binding affinity of PD-L1 aptamers. The binding affinity of PD-L1 aptamers to cancer cell lines was assessed by flow cytometry.

H1975, A549 and B16F10 cells were imaged by confocal microscopy (Figure 3). A strong fluorescence signal was detected on the plasma membrane of PD-L1-positive H1975 and B16F10 cells. Specifically, the 2198-06-07 PD-L1 aptamer showed the strongest fluorescence signal intensity. In contrast,

PD-L1-negative A549 cells showed undetectable fluorescence of the PD-L1 aptamers.

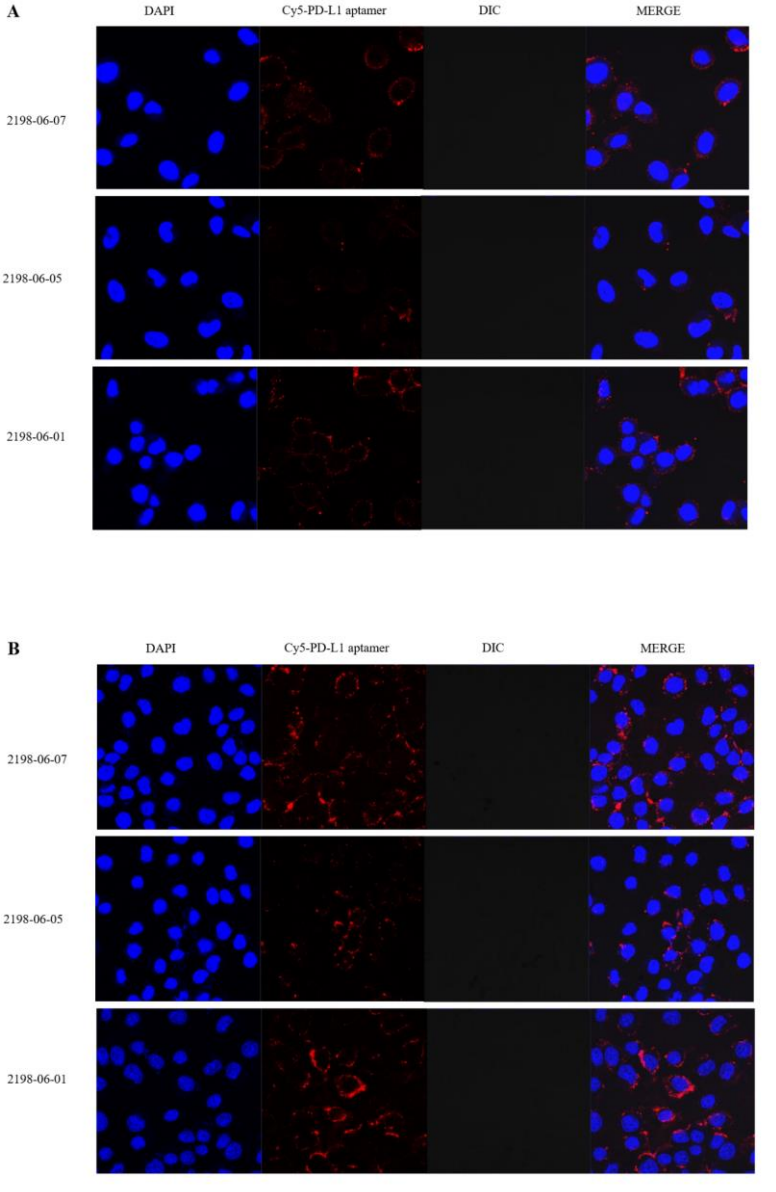

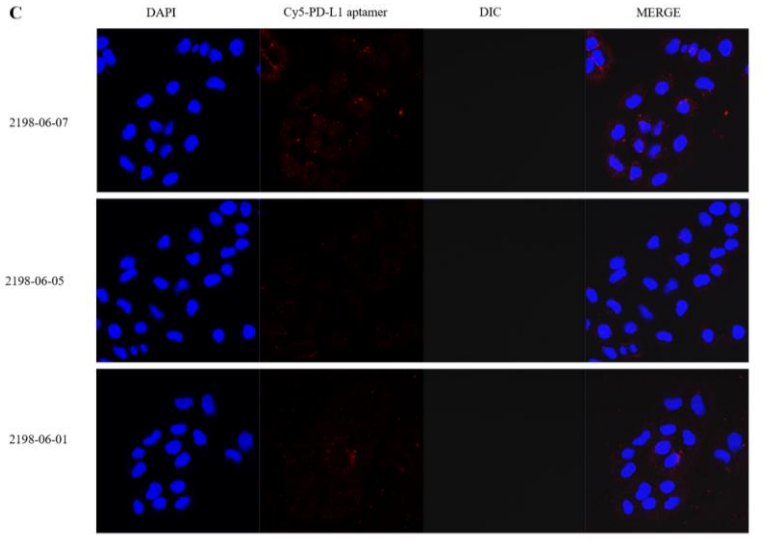

Figure 3. Confocal microscopy images of PD-L1 aptamers in tumor cells. H1975 (A), B16F10 (B), and A549 (C), incubated with three Cy5-labeled PD-L1 aptamers (red). PD-L1 was stained with DAPI (blue).

To further investigate the binding specificity of PD-L1 aptamers, flow cytometry and confocal microscopy were performed on H1975 cells using a scrambled aptamer as a negative control, and a large amount of PD-L1 aptamer was used for the blocking assay (Figure 4). In both studies, the scrambled aptamer did not bind to H1975 cells, but the 2198-06-07 PD-L1 aptamer was bound to H1975 cells. In the blocking study, we confirmed that the PD-L1 aptamer did not bind after treatment with a large amount of aptamer.

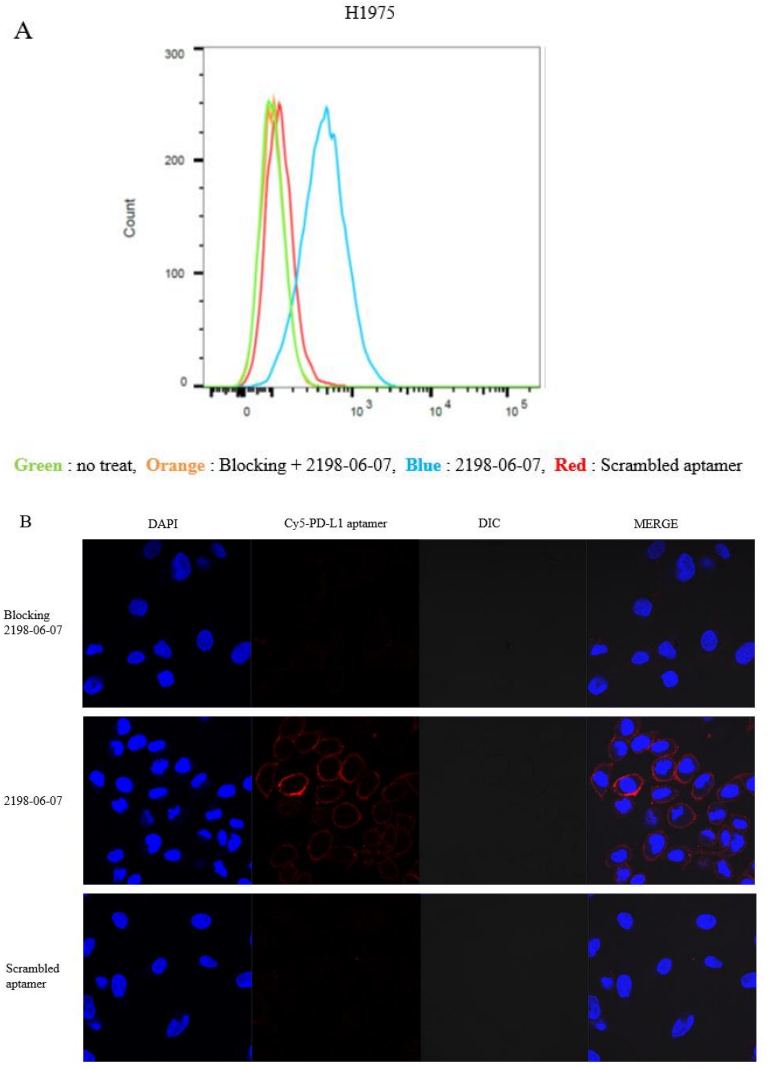

Figure 4. Flow cytometry (A) and confocal microscopy images (B) of scrambled aptamer, 2198-06-07 PD-L1 aptamer and blocking assay

To determine whether PD-L1 aptamers were internalized after binding to the cell-surface target, z-stack images of H1975 and A549 cells were evaluated. Confocal z-stack imaging of 5'-Cy5-2198-06-07 PD-L1 aptamers over a 4-h period indicated that 2198-06-07 PD-L1 aptamers were efficiently internalized

into H1975 cells. However, 2198-06-07 PD-L1 aptamers were not internalized into A549 cells (Figure 5).

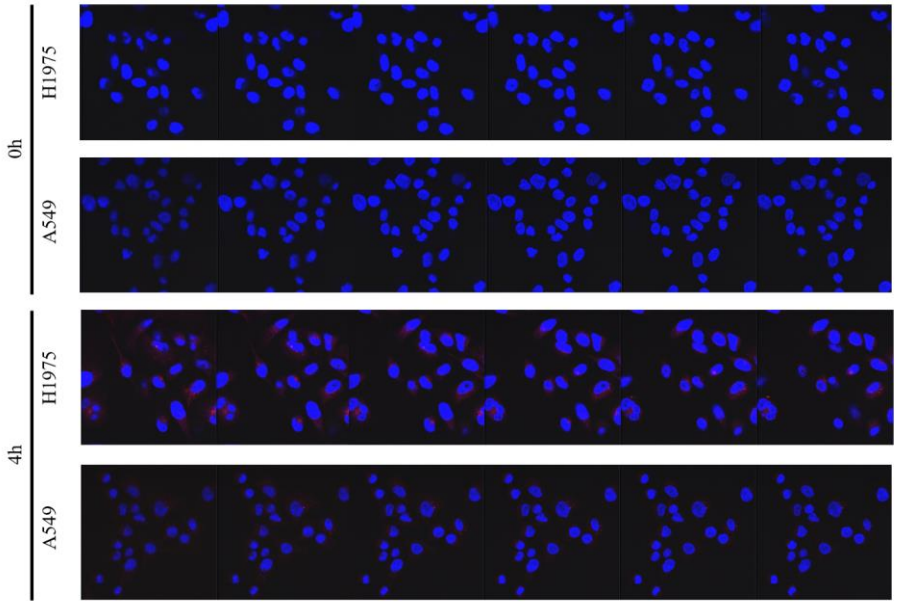

Figure 5. Internalization of PD-L1 aptamers. Representative confocal z stack images of H1975 and A549 cells incubated with the 5'-Cy5-2198-06-07 PD-L1 aptamer.

3. Optical imaging of PD-L1 aptamers in H1975 tumor bearing mice

Figure 6 shows fluorescent images of H1975 tumor bearing mice after the intravenous injection of 1 nmol of Cy5-PD-L1 aptamers. The H1975 tumors were clearly visualized from the background tissue. H1975 tumor-bearing mice were sacrificed, and the major organs and tumors were collected 60 min after injection. A quantification analysis of tumors was performed and the signal intensity of the 2198-06-01 PD-L1 aptamer of the H1975 tumor was 1.15×10^9 [photons/sec/cm^2/sr]/[μW/cm^2] while that of the 2198-06-05 PD-L1 aptamer was

9.68 × 10^8 [photons/sec/cm^2/sr]/[μW/cm^2]. The 2198-06-07 PD-L1 aptamer showed the highest signal intensity (2.30 × 10^9 [photons/sec/cm^2/sr]/[μW/cm^2]).

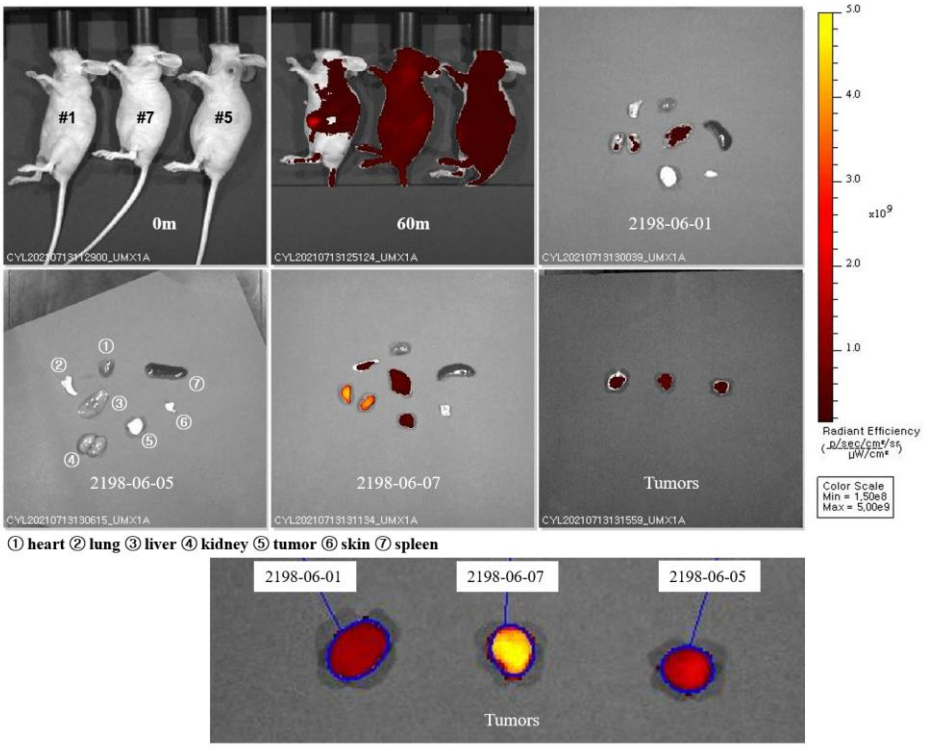

Figure 6. *In vivo* and *ex vivo* fluorescence imaging of PD-L1 aptamers in H1975 tumor bearing mice.

4. *In vivo* PET scanning

The 2198-06-07 PD-L1 aptamer showed the highest affinity for PD-L1-positive cells and tumors. The 2198-06-07 PD-L1 aptamer was radiolabeled with ^{68}Ga. Using microPET, *in vivo* molecular images of H1975 and A549 tumor-bearing mice were taken 30 min after the injection of ^{68}Ga-NOTA-PD-L1 aptamers. The PET images of the H1975 tumor-bearing mice presented a significantly greater accumulation of ^{68}Ga-NOTA-PD-L1 aptamers in the tumor than than that of A549 tumor-bearing mice (Figure 7). In addition to the tumor, a high uptake of

^{68}Ga-NOTA-PD-L1 aptamers was detected in the kidneys, which are involved in tracer excretion.

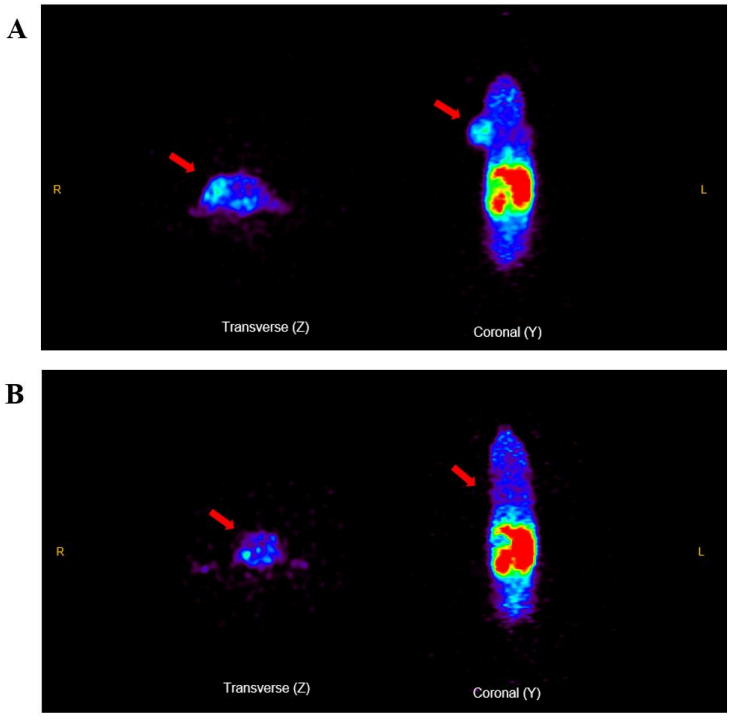

Figure 7. MicroPET images of ^{68}Ga-NOTA-PD-L1 aptamers in tumor bearing mice. Representative static PET images at 30 min after the injection of ^{68}Ga-NOTA-PD-L1 aptamers (A: H1975 tumor, B: A549 tumor)

To further investigate the uptake of ^{68}Ga-NOTA-PD-L1 aptamers on tumors with different PD-L1 expression, the two tumors (H1975 and A549) were implanted in a mouse. Representative microPET images of dual tumor-bearing (H1975 and A549) mice after the administration of ^{68}Ga-NOTA-PD-L1 aptamers are presented in Figure 8. The ^{68}Ga-NOTA-PD-L1 aptamers clearly resolved the H1975 tumor. Moreover, there was no visible accumulation of

^{68}Ga-NOTA-PD-L1 aptamers in the A549 tumor. The SUVmax of the H1975 tumor was 4.16 and that of the A549 tumor was 1.18 (Figure 8).

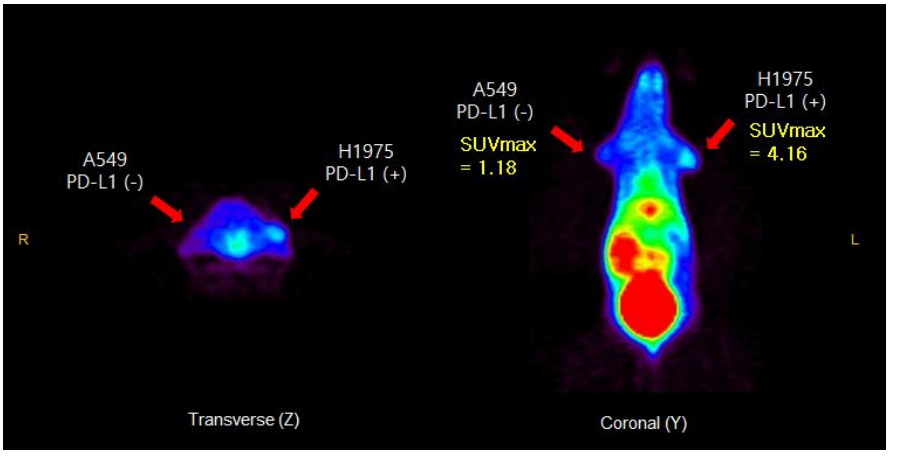

Figure 8. MicroPET images of ^{68}Ga-NOTA-PD-L1 aptamers in dual (H1975 and A549) tumor-bearing mice. Representative static PET images at 30 min after injection of ^{68}Ga-NOTA-PD-L1 aptamers

We obtained dynamic microPET images of dual tumor-bearing (H1975 and A549) mice after ^{68}Ga-NOTA-PD-L1 aptamer injection. The serial microPET images of the ^{68}Ga-NOTA-PD-L1 aptamer at different time points are shown in Figure 9. The ^{68}Ga-NOTA-PD-L1 aptamer uptake of the H1975 tumor was higher than that of the A549 tumor at all time points. Quantitative analysis approved that the highest tumor uptake was observed after 30 min.

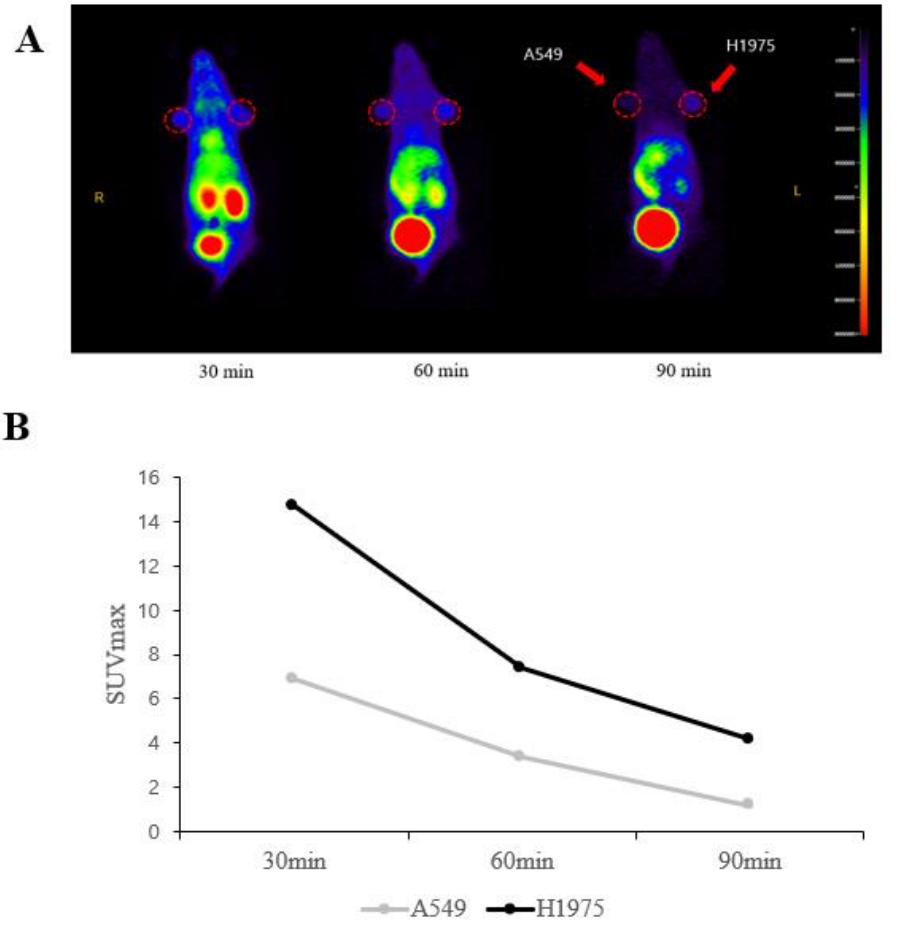

Figure 9. Dynamic microPET images of ^{68}Ga-NOTA-PD-L1 aptamers in dual (H1975 and A549) tumor-bearing mice. (A) Representative coronal microPET images of dual tumor-bearing (H1975 and A549) mice at 30, 60, and 90 min after ^{68}Ga-NOTA-PD-L1 aptamer administration. (B) The quantitative analysis of ^{68}Ga-NOTA-PD-L1 aptamer microPET images of dual tumor-bearing (H1975 and A549) mice

5. Biodistribution

The tissue biodistribution of the ^{68}Ga-NOTA-PD-L1 aptamers was evaluated in the H1975 tumor-bearing mice. We observed a consistently low background signal in most of the collected organs, including the blood, heart, lung, spleen, stomach, large intestine, muscle, and femur (Figure 10). The highest uptake was observed in the kidneys at 30 min (4.14 ± 1.01 %ID/g), and it decreased 60 min after the injection (2.58 ± 0.61%ID/g). The tumor uptake was higher 30 min after injection (% ID/g = 0.91%) than at 60 min after the injection (% ID/g = 0.43%). The blood uptake of ^{68}Ga-NOTA-PD-L1 aptamers was 0.75 ± 0.28 %ID/g at 30 min, which decreased to 0.45 ± 0.17%ID/g at 60 min after injection.

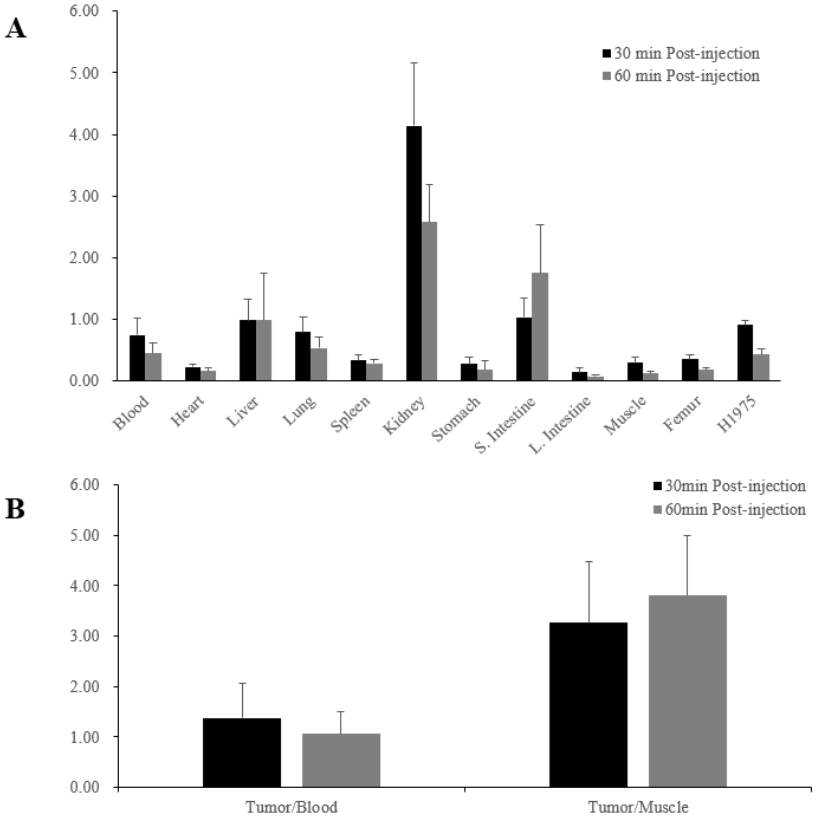

Figure 10. Biodistribution of the ^{68}Ga-NOTA-PD-L1 aptamer. (A) The uantitative analysis of the biodistribution of the ^{68}Ga-NOTA-PD-L1 aptamer. Radioactivity is expressed as %ID/g. (B) Tumor/blood and tumor/muscle ratios of the ^{68}Ga-NOTA-PD-L1 aptamer at each time.

IV. DISCUSSION

The aim of present study was to develop a ^{68}Ga-NOTA-PD-L1 aptamer and investigate its target specificity and utility for *in vivo* PET scanning. The PD-L1-specific aptamer is an attractive molecule for PET scanning with a high affinity for its target. We successfully produced a radiolabeled ^{68}Ga-NOTA-PD-L1 aptamer and obtained PET images *in vivo*.

Since the SELEX method was developed, numerous SELEX variants have been modified and novel aptamers have been identified[15,16]. Aptamers are oligomers composed of ribonucleotides, deoxynucleotides, or amino acids. Aptamers can develop three-dimensional structures that enable them to bind to specific targets[17]. Aptamers have many advantages over large molecules, including antibodies. First, aptamers have a relatively small size (5–15 kDa) in comparison to antibodies[18], meaning that they can penetrate tissues and tumors faster than antibodies. Unlike antibodies, aptamers can be designated for most targets and are generally poorly immunogenic and non-toxic[19]. In addition, aptamers are chemically synthesized and structurally easy to modify. Therefore, aptamers can be produced in bulk at a relatively low cost, customized, and modified for numerous applications, including molecular imaging, biomarker discovery, and drug development[20,21].

PD-1 plays an essential role in the regulating of immune response to tumor antigens and autoantigens. PD-1 is a co-inhibitory molecule for T-cell receptor signaling that is expressed on activated T-cells. Its ligand, PD-L1, is expressed in both cancer cells and tumor-infiltrating lymphocytes. Binding of PD-1/PD-L1

suppresses T cell function and the axis is thought to be a major pathway involved in tumor immune evasion[22]. PD-1/PD-L1 block by monoclonal antibodies has confirmed to be efficient for overcoming immune evasion and mobilizing specific antitumor responses in mouse models and clinically in patients[23,24]. Monoclonal antibodies have been applied in the clinical setting to inhibit the activity of specific proteins, including PD-L1[25,26]. However, monoclonal antibody therapies have several restrictions, such as high immunogenicity and production cost[27,28]. In contrast, aptamers lack immunogenicity and can be synthesized at a low cost[29-31]. As mentioned above, aptamers can also be rapidly recognized to attach molecular targets, such as PD-L1, with high affinity and specificity. Therefore, PD-L1 aptamers are promising candidates for molecular imaging and targeted therapy.

Despite the promising development of PD-L1 inhibitors as anticancer agents, predicting PD-L1 expression in cancer remains a challenge. The most widely used method for predicting PD-L1 expression is IHC. However, there are several concerns about evaluating PD-L1 expression by IHC assay, particularly with regard to its true predictability due to high variability, heterogeneity, and dynamic expression in tumors. Thus, the identification of ideal biomarkers for PD-L1 expression is important.

Nuclear imaging techniques, such as PET and SPECT, allow the visualization of specific physiological, biochemical, and functional changes. The successful application of aptamer-based nuclear imaging has been established with ^{99m}Tc-labeled tenascin-C and MUC1-targeted aptamers and ^{18}F-labeled HER2-aptamers[32-34]. Most PET studies have focused on the use of four ordinary radionuclides: ^{18}F, ^{11}C, ^{13}N, and ^{15}O. However, the rapid decay of ^{11}C, ^{13}N, and ^{15}O induces several limitations of the types of chemistry that can be used for the preparation of radiopharmaceuticals. ^{18}F has several advantages, but it is produced by a cyclotron. Therefore, alternative radionuclides with varying physical properties were investigated. ^{68}Ga is an attractive alternative to ^{18}F for

radiolabeling low-molecular-weight molecules, which generally demonstrate rapid pharmacokinetics[35]. In clinical practice, ^{68}Ga can be produced using a convenient ^{68}Ge/^{68}Ga generator system. ^{68}Ga serves as a low-cost alternative to cyclotron-produced PET radionuclides[12,36]. In this study, we radiolabeled the PD-L1 aptamer with ^{68}Ga and obtained PET images *in vivo*. To our knowledge, the present study is the first to report PD-L1-specific ^{68}Ga-labeled PET scanning using a PD-L1 aptamer. PET images of PD-L1 positive tumor-bearing mice presented reliable tumor-to-background ratios, implying that the aptamer identified PD-L1 *in vivo*. PET scanning may provide as a predictive biomarker for selecting patients for anti-PD-1/PD-L1 immune checkpoint inhibitor therapy. Furthermore, it also holds potential for the longitudinal assessment of therapy response.

This study has several limitations. In the tumor microenvironment, infiltrating immune cells also express PD-L1, in addition to tumor cells. We did not evaluate the contribution of the PET signals. Second, we did not evaluate the efficacy of the ^{68}Ga-NOTA-PD-L1 aptamers for cancer treatment. We only collected basic information on the biodistribution and *in vivo* PET scanning. Aptamers are attractive therapeutic agents because of their high target binding affinity and low toxicity. However, few aptamers have been reported for use in aptamer-based cancer therapies. Rapid renal excretion and degradation by nucleases are the major drawbacks of aptamers as therapeutic agents. Further studies are necessary to evaluate the therapeutic utility of ^{68}Ga-NOTA-PD-L1 aptamers.

V. CONCLUSION

^{68}Ga-NOTA-PD-L1 aptamers facilitated the visualization of PD-L1 expression by *in vivo* PET scanning. These promising results suggest that radiolabeled PD-L1 aptamers may have potential applications as diagnostic agents and for use in determining strategies for the immunotherapy of PD-L1 positive cancers.

REFERENCES

1. Zou W, Wolchok JD, Chen L. PD-L1 (B7-H1) and PD-1 pathway blockade for cancer therapy: Mechanisms, response biomarkers, and combinations. Sci Transl Med 2016;8:328rv4.
2. Agata Y, Kawasaki A, Nishimura H, Ishida Y, Tsubata T, Yagita H, et al. Expression of the PD-1 antigen on the surface of stimulated mouse T and B lymphocytes. Int Immunol 1996;8:765-72.
3. Gato-Canas M, Zuazo M, Arasanz H, Ibanez-Vea M, Lorenzo L, Fernandez-Hinojal G, et al. PDL1 Signals through Conserved Sequence Motifs to Overcome Interferon-Mediated Cytotoxicity. Cell Rep 2017;20:1818-29.
4. Pardoll DM. The blockade of immune checkpoints in cancer immunotherapy. Nat Rev Cancer 2012;12:252-64.
5. Meng X, Huang Z, Teng F, Xing L, Yu J. Predictive biomarkers in PD-1/PD-L1 checkpoint blockade immunotherapy. Cancer Treat Rev 2015;41:868-76.
6. Peng J, Hamanishi J, Matsumura N, Abiko K, Murat K, Baba T, et al. Chemotherapy Induces Programmed Cell Death-Ligand 1 Overexpression via the Nuclear Factor-kappaB to Foster an Immunosuppressive Tumor Microenvironment in Ovarian Cancer. Cancer Res 2015;75:5034-45.
7. Zhang P, Su DM, Liang M, Fu J. Chemopreventive agents induce programmed death-1-ligand 1 (PD-L1) surface expression in breast cancer cells and promote PD-L1-mediated T cell apoptosis. Mol Immunol 2008;45:1470-6.
8. Mayer G. The chemical biology of aptamers. Angew Chem Int Ed Engl 2009;48:2672-89.
9. Sun H, Zhu X, Lu PY, Rosato RR, Tan W, Zu Y. Oligonucleotide aptamers: new tools for targeted cancer therapy. Mol Ther Nucleic Acids

2014;3:e182.

10. Lao YH, Phua KK, Leong KW. Aptamer nanomedicine for cancer therapeutics: barriers and potential for translation. ACS Nano 2015;9:2235-54.
11. James ML, Gambhir SS. A molecular imaging primer: modalities, imaging agents, and applications. Physiol Rev 2012;92:897-965.
12. Prata MI. Gallium-68: a new trend in PET radiopharmacy. Curr Radiopharm 2012;5:142-9.
13. Martiniova L, Palatis L, Etchebehere E, Ravizzini G. Gallium-68 in Medical Imaging. Curr Radiopharm 2016;9:187-207.
14. Gijs M, Dammicco S, Warnier C, Aerts A, Impens NR, D'Huyvetter M, et al. Gallium-68-labelled NOTA-oligonucleotides: an optimized method for their preparation. J Labelled Comp Radiopharm 2016;59:63-71.
15. Stoltenburg R, Reinemann C, Strehlitz B. SELEX--a (r)evolutionary method to generate high-affinity nucleic acid ligands. Biomol Eng 2007;24:381-403.
16. Spiridonova VA, Kopylov AM. DNA aptamers as radically new recognition elements for biosensors. Biochemistry (Mosc) 2002;67:706-9.
17. Lakhin AV, Tarantul VZ, Gening LV. Aptamers: problems, solutions and prospects. Acta Naturae 2013;5:34-43.
18. Lee JW, Kim HJ, Heo K. Therapeutic aptamers: developmental potential as anticancer drugs. BMB Rep 2015;48:234-7.
19. Shigdar S, Lin J, Yu Y, Pastuovic M, Wei M, Duan W. RNA aptamer against a cancer stem cell marker epithelial cell adhesion molecule. Cancer Sci 2011;102:991-8.
20. Ni X, Castanares M, Mukherjee A, Lupold SE. Nucleic acid aptamers: clinical applications and promising new horizons. Curr Med Chem 2011;18:4206-14.
21. Tan W, Donovan MJ, Jiang J. Aptamers from cell-based selection for bioanalytical applications. Chem Rev 2013;113:2842-62.

22. Gong J, Chehrazi-Raffle A, Reddi S, Salgia R. Development of PD-1 and PD-L1 inhibitors as a form of cancer immunotherapy: a comprehensive review of registration trials and future considerations. J Immunother Cancer 2018;6:8.

23. Hirano F, Kaneko K, Tamura H, Dong H, Wang S, Ichikawa M, et al. Blockade of B7-H1 and PD-1 by monoclonal antibodies potentiates cancer therapeutic immunity. Cancer Res 2005;65:1089-96.

24. Callahan MK, Wolchok JD. At the bedside: CTLA-4- and PD-1-blocking antibodies in cancer immunotherapy. J Leukoc Biol 2013;94:41-53.

25. Deng R, Bumbaca D, Pastuskovas CV, Boswell CA, West D, Cowan KJ, et al. Preclinical pharmacokinetics, pharmacodynamics, tissue distribution, and tumor penetration of anti-PD-L1 monoclonal antibody, an immune checkpoint inhibitor. MAbs 2016;8:593-603.

26. Stewart R, Morrow M, Hammond SA, Mulgrew K, Marcus D, Poon E, et al. Identification and Characterization of MEDI4736, an Antagonistic Anti-PD-L1 Monoclonal Antibody. Cancer Immunol Res 2015;3:1052-62.

27. Nelson AL, Dhimolea E, Reichert JM. Development trends for human monoclonal antibody therapeutics. Nat Rev Drug Discov 2010;9:767-74.

28. Harding FA, Stickler MM, Razo J, DuBridge RB. The immunogenicity of humanized and fully human antibodies: residual immunogenicity resides in the CDR regions. MAbs 2010;2:256-65.

29. White RR, Sullenger BA, Rusconi CP. Developing aptamers into therapeutics. J Clin Invest 2000;106:929-34.

30. Keefe AD, Pai S, Ellington A. Aptamers as therapeutics. Nat Rev Drug Discov 2010;9:537-50.

31. Chang YM, Donovan MJ, Tan W. Using aptamers for cancer biomarker discovery. J Nucleic Acids 2013;2013:817350.

32. Daniels DA, Chen H, Hicke BJ, Swiderek KM, Gold L. A tenascin-C

aptamer identified by tumor cell SELEX: systematic evolution of ligands by exponential enrichment. Proc Natl Acad Sci U S A 2003;100:15416-21.

33. Pieve CD, Perkins AC, Missailidis S. Anti-MUC1 aptamers: radiolabelling with (99m)Tc and biodistribution in MCF-7 tumour-bearing mice. Nucl Med Biol 2009;36:703-10.

34. Kim HJ, Park JY, Lee TS, Song IH, Cho YL, Chae JR, et al. PET imaging of HER2 expression with an 18F-fluoride labeled aptamer. PLoS One 2019;14:e0211047.

35. Banerjee SR, Pomper MG. Clinical applications of Gallium-68. Appl Radiat Isot 2013;76:2-13.

36. Velikyan I. 68Ga-Based radiopharmaceuticals: production and application relationship. Molecules 2015;20:12913-43.

ABSTRACT (IN KOREAN)

암 PD-L1 발현여부 평가를 위한 압타머 개발

<지도교수 강원준>

연세대학교 대학원 의학과

최윤정

배경: Programmed death-1 (PD-1) 수용체는 활성화된 T 세포에서 발현되는 면역 억제 수용체이며 리간드인 PD-L1와 결합하여 말초 조직에서 T 림프구 기능을 조절한다. 최근 연구에 따르면 PD-1 또는 PD-L1에 대한 단클론항체를 이용하여 그 기능을 억제하여 종양특이 T 림프구 세포활성 및 효과를 증강시켜 항종양 면역을 향상시킬 수 있다. 따라서 PD-1/PD-L1 axis는 암 면역 요법의 잠재적인 치료 옵션이 될 수 있다. 압타머는 표적 분자에 대해 높은 특이성과 친화성을 갖는 올리고뉴클레오티드로서 항체와 비슷한 성질을 보이지만 면역반응이 없어 분자 영상화 및 표적 치료를 위한 유망한 후보 물질로 각광받고 있다. ^{68}Ga는 사이클로트론에서 생산되는 PET 방사성 핵종으로 경제성이 뛰어나고 표지가 매우 간편하여 앞으로 ^{18}F을 대체할 만한 매력적인 PET 방사성 핵종이다. 이 연구에서 우리는 ^{68}Ga로 표지된 PD-L1 압타머를 개발하고 생체 내 PET 이미징을 위한 표적 특이성과 유용성을 조사했다.

방법: PD-L1 압타머의 결합 친화도를 알기 위하여 3가지 종류의 PD-L1 압타머와 PD-L1 양성 종양 세포 (H1975, B16F10), PD-L1 음성 종양 세포 (A549, HT-29)에서 친화도를 공초점레이저 현미경을 통해 평가하였다. 3가지 압타머 중 가장 친화도가 높은 압타머에

^{68}Ga로 방사성 표지하여 ^{68}Ga-NOTA-PD-L1 압타머를 합성하였다. 그 후 H1975 종양모델과 A549 종양모델에 ^{68}Ga-NOTA-PD-L1 압타머를 정맥주사하고 양전자 방출 단층 촬영(PET)을 시행하였다.

결과: 유세포 분석 및 공초점 현미경 검사에서 PD-L1 압타머는 PD-L1 양성 세포인 H1975 및 B16F10 세포에 강한 친화도를 보였다. 대조적으로, PD-L1 음성 세포인 A549 및 HT-29 세포는 PD-L1 압타머에 대해 낮은 친화도를 보였다. 3가지 PD-L1 압타머 중 2198-06-07-PD-L1-압타머가 가장 높은 친화도를 보여 2198-06-07-PD-L1-압타머를 ^{68}Ga으로 표지하여 ^{68}Ga-NOTA-PD-L1 압타머를 합성하였다. 68Ga-NOTA-PD-L1 압타머의 PET 영상은 A549 종양모델에 비해 PD-L1 양성 H1975 종양모델에서 증가된 섭취를 보여주었다.

결론: ^{68}Ga-NOTA-PD-L1-압타머는 in vivo PET을 통해 PD-L1 발현을 영상화할 수 있었다. 이러한 결과는 ^{68}Ga-NOTA-PD-L1 압타머가 잠재적으로 PD-L1 양성 종양의 진단과 치료군 설정에 임상적 활용 가능성이 있음을 시사한다.

핵심되는 말 : 압타머, PD-L1, ^{68}Ga, 분자영상